Adaptive Threshold Optimization for a Blanking Nonlinearity in OFDM Receivers

Ulrich Epple
Institute of Communications and Navigation
German Aerospace Center (DLR)
Email: ulrich.epple@dlr.de

Michael Schnell
Institute of Communications and Navigation
German Aerospace Center (DLR)
Email: michael.schnell@dlr.de

***Abstract*—The application of a blanking nonlinearity to cope with impulsive interference is a common approach in OFDM systems. The choice of the amplitude threshold to decide whether a received sample is blanked, heavily affects the performance of the entire transmission. As a matter of fact, the perfect blanking threshold strongly depends on the characteristics of the interference. In previous publications this perfect threshold has been derived, given knowledge about the interference statistics. In general, however, no reliable information about the interference statistics is known at the receiver side. In this paper a practical method for calculating an adaptive blanking threshold to maximize the signal-to-interference-and-noise ratio after the blanking nonlinearity is proposed. The calculation is based on the distribution of the amplitude of the received signal at the OFDM receiver. Simulation results show only a negligible performance degradation when comparing the proposed method to the case where the theoretically derived perfect threshold is applied for blanking.**

I. Introduction

In the past years, orthogonal frequency division multiplexing (OFDM) has been established as modulation technique that is employed in numerous systems for wireless and wired communications, for example digital video broadcasting (DVB) or powerline communications (PLC). It provides several advantages compared to single-carrier systems, such as spectral efficiency, robustness to multipath propagation, and its efficient implementation by a fast Fourier transform (FFT), just to mention a few.

Besides multipath propagation effects and additive white Gaussian noise (AWGN), these systems are often exposed to impulsive interference, e.g. originating from switching processes on the power distribution network or from the ignitions of passing vehicles, leading to a degradation of the system performance [1]. Due to its non-Gaussian nature, this interference has to be represented by specific impulsive interference models [2]–[4].

For moderate impulsive interference power and infrequent occurrence, OFDM systems can cope well with the interference, as it is spread among several sub-carriers of an OFDM symbol. However for frequent occurrence or high interference power, this spread will turn into a disadvantage [2] and interference mitigation techniques have to be implemented.

Many approaches to mitigate the impact of impulsive interference are based on applying a memoryless blanking nonlinearity (BN) at the receiver input, prior to the OFDM demodulator, such as [5]–[8].

In our investigations we will focus on this BN since it is easy to implement, while providing a remarkable performance gain, compared to a conventional OFDM receiver [6]. The crucial parameter for setting up the BN is the blanking threshold which determines whether a received sample is blanked or not. This value has to be chosen properly, as it is a trade-off between removing interference and preserving the useful OFDM signal. In [9] it was shown that a perfect threshold always exists, which depends on the parameters of the impulsive interference. Furthermore, an expression for obtaining this perfect blanking threshold was derived. However, these considerations are based on knowledge about the impulsive interference statistics, which, in general, is not known at the receiver side.

In this paper, we propose a method for calculating an adaptive blanking threshold without any information about the actual impulsive interference. The calculation is based on measurements of the amplitude distribution of the received signal at the OFDM receiver. The obtained threshold is optimal in terms of maximizing the signal-to-noise-and-interference ratio (SINR) after the BN. Simulation results indicate that the perfect threshold is nearly achieved and only a negligible performance loss is introduced.

In addition, we will examine the influence of the FFT size on the performance of our proposed algorithm. Finally, we will show that, depending on the interference model, the calculation of a separate threshold for each OFDM symbol is more appropriate compared to an average threshold for multiple OFDM symbols. Our results can be directly applied to practical applications, when applying a BN.

The paper is organized as follows. In Section II, the considered system model is introduced. In Section III, we present our algorithm for deriving the adaptive blanking threshold. This is followed by Section IV, where the performance of our proposed algorithm is compared to result with the theoretically perfect threshold from [9]. In Section V, we address the influence of the FFT size and the chosen interference model. Finally, the paper is concluded in Section VI.

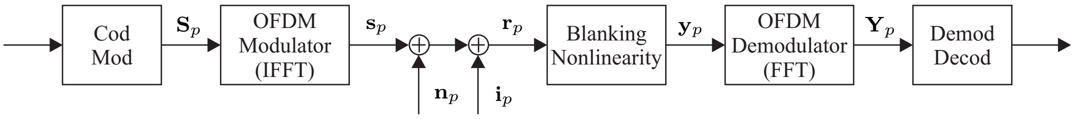

Fig. 1. System model for an OFDM transmission with a blanking nonlinearity.

II. System Model

For our investigation we consider the digital baseband model from Fig. 1. A stream of source bits enter a coding and modulation block, incorporating channel coding of the source bits and mapping onto modulation symbols using a quadrature phase shift keying (QPSK) modulation alphabet. N modulated symbols $S_k, k = 0, 1, ..., N-1$ are arranged in a vector[1] $\mathbf{S}_p = [S_{p,0}, S_{p,1}, ..., S_{p,N-1}]^T$ to form an OFDM symbol with the OFDM symbol denoted by a subscript index p. The latter is then transformed into the time domain using an inverse fast Fourier transform (IFFT) to obtain the transmit vector $\mathbf{s}_p = [s_{p,0}, s_{p,1}, ..., s_{p,N-1}]^T$. As we focus only on an additive channel model, the common insertion of a guard interval (GI) to prevent inter-symbol interference (ISI) is, without loss of generality, omitted for simplicity.

The transmit vector passes an additive transmission channel, including AWGN $\mathbf{n}_p = [n_{p,0}, n_{p,1}, ..., n_{p,N-1}]^T$ and impulsive interference $\mathbf{i}_p = [i_{p,0}, i_{p,1}, ..., i_{p,N-1}]^T$. Finally, the model of the received signal can be represented as

$$\mathbf{r}_p = \mathbf{s}_p + \mathbf{n}_p + \mathbf{i}_p, \tag{1}$$

where $\mathbf{r}_p = [r_{p,0}, r_{p,1}, ..., r_{p,N-1}]^T$ denotes an N-point vector of received samples. The signals $\mathbf{s}_p$, $\mathbf{n}_p$, and $\mathbf{i}_p$ are assumed to be statistically independent; we further assume without loss of generality that the power of the transmitted signal is normalized to one, i.e. $E\left\{|s_{p,l}|^2\right\} = 2\sigma_s^2 = 1$, with l denoting the sample index in the time domain. When using a normalized FFT, $E\left\{|S_{p,k}|^2\right\} = 1$ holds as well. In this context k is defined as the sub-carrier index. For the average power of the AWGN samples it holds $N_0 = 2\sigma_n^2$. The parameters σ_s^2 and σ_n^2 are the component-wise variance of the transmit and the noise signal, respectively.

In this study, we consider two types of impulsive interference. The first is a Bernoulli-Gaussian process [2] defined as

$$i_{p,l} = b_{p,l} \cdot g_{p,l}, \tag{2}$$

where $b_{p,l}$ is the Bernoulli process and the distribution of the samples $g_{p,l}$ is characterized by a zero mean, complex Gaussian process. The impulsive interference is described by the probability $\mathcal{P}(b_{p,l} = 1) = \beta$ and the component-wise variance of $g_{p,l}$, $\sigma_g^2 = 1/2\, E\left\{|g_{p,l}|^2\right\}$. This scheme has already been used in various studies, e.g. [2], [9] to assess the influence of impulsive interference.

As investigated in [4], many sources of impulsive noise do not occur as single peaks, as described by the Bernoulli-Gaussian process, but rather as bursts with a certain duration. This can be modeled by Gated-Gaussian noise [4], which was also considered for the investigations in [10]. Like for the Bernoulli-Gaussian process, the Gated-Gaussian process can be described by (2). For Gated-Gaussian noise, the term $g_{p,l}$ is also characterized by a zero mean, complex Gaussian process with the same definition of the variance σ_g^2. In contrast to the Bernoulli-Gaussian model, the occurrence of the Gated-Gaussian noise is described by two variables. The first is the fraction of time of an OFDM symbol μ, during which the Gated-Gaussian noise occurs. This translates into N_μ affected samples in the digital baseband model, calculated by

$$N_\mu = \lfloor \mu N + 1/2 \rfloor. \tag{3}$$

Obviously, these samples occur as a contiguous block. As the noise burst may only occur rarely, a second parameter ν is defined, which determines that only every ν-th OFDM symbol is affected by an interference burst. This writes mathematically

$$b_{p,l} = \begin{cases} 1, & \text{if} \quad p \bmod \nu = 0 \quad \wedge \\ & l = l_{0,p}, l_{0,p}{+}1, ..., l_{0,p}{+}N_\mu{-}1, \\ 0, & \text{else}, \end{cases} \tag{4}$$

with $l_{0,p}$ being randomly chosen numbers from $[0, 1, ..., N - N_\mu]$.

In order to remove high peaks of the impulsive interference, a BN is applied which is described later on. Following the nonlinearity, the blanked signal $\mathbf{y}_p = [y_{p,0}, y_{p,1}, ..., y_{p,N-1}]^T$ is transformed into the frequency domain by means of an FFT which results in the frequency domain signal $\mathbf{Y}_p = [Y_{p,0}, Y_{p,1}, ..., Y_{p,N-1}]^T$. Finally, $\mathbf{Y}_p$ passes a soft-demodulator to obtain soft values of the encoded bits, which are fed into the decoder, leading to estimates of the transmitted source bits.

The BN is described by the memoryless nonlinear mapping $f : \mathbb{C} \rightarrow \mathbb{C}$ specified as follows:

$$y_{p,l} = f(r_{p,l}) = \begin{cases} r_{p,l}, & \text{if} \quad |r_{p,l}| < T_{\mathrm{BN}}, \\ 0, & \text{else}, \end{cases} \tag{5}$$

where T_{BN} is the blanking threshold. The perfect blanking threshold value depends on the interference model. In former investigations [7], [11], [12], a fixed predefined threshold is selected, which is chosen according to the expected interference situation. In contrast, we propose to apply an adaptive threshold, based on the amplitude distribution of the received samples. It is calculated such as to maximize the SINR after the BN. Therefore, we will show how this SINR can be estimated, in dependence of the blanking threshold. In what follows, we describe in detail the algorithm for calculating the adaptive threshold.

[1]Herein, column vectors are written as bold letters; capital letters denote signals in the frequency domain, small letters time domain signals.

III. Proposed Algorithm

In this section, we show how an optimal threshold for the BN can be calculated. The principle of the algorithm is to estimate the SINR after the BN, which depends on the blanking threshold T_{BN}. By maximizing this SINR, i.e., searching for the T_{BN} which leads to the highest SINR, one obtains the optimal blanking threshold

$$T_{\mathrm{BN,opt}} = \arg\left(\max\left(\mathrm{SINR}(T_{\mathrm{BN}})\right)\right), \quad T_{\mathrm{BN}} > 0. \tag{6}$$

For deriving an expression for the $\mathrm{SINR}(T_{\mathrm{BN}})$, we will first introduce two parameters.

The first is the expectation value of the remaining impulsive interference power $P_{\mathrm{I}}(T_{\mathrm{BN}})$ at a sub-carrier after the BN. Obviously, there will be received samples comprising impulsive interference, however with an amplitude below the threshold. These samples cause the remaining interference power $P_{\mathrm{I}}(T_{\mathrm{BN}})$.

Secondly we introduce the factor $K(T_{\mathrm{BN}})$, which is defined as the ratio of the expected sub-carrier OFDM and AWGN power after and before the BN. In [13] it was shown that the power of the OFDM signal at a certain sub-carrier when applying a BN consists of two parts. The first part is the attenuated useful signal power of the transmitted symbol at this sub-carrier. The second part is undesired inter-carrier interference (ICI) from the other sub-carriers, which is induced by the BN. In [13] it was also shown that the power of the useful part is $K^2(T_{\mathrm{BN}})$ and the ICI power is $K(T_{\mathrm{BN}})(1-K(T_{\mathrm{BN}}))$ for $E\left\{|S_{p,k}|^2\right\} = 1$.

Keeping the different parts of the signal after the BN in mind, the sub-carrier SINR after the BN can now be calculated by

$$\mathrm{SINR}(T_{\mathrm{BN}}) = \\ = \frac{K^2(T_{\mathrm{BN}})}{K(T_{\mathrm{BN}})N_0 + K(T_{\mathrm{BN}})(1-K(T_{\mathrm{BN}})) + P_{\mathrm{I}}(T_{\mathrm{BN}})}. \tag{7}$$

The numerator consists of the remaining useful OFDM signal power. The denominator comprises the attenuated noise term, ICI which is induced by the BN, and the remaining impulsive interference. Note that (7) was already derived in [13], however without P_{I}, which was neglected in this context.

The calculation of the SINR according to (7) is based on some assumptions, which will be summarized in the following. The AWGN and the impulsive interference are still white after the BN, i.e., comprise a flat power spectral density since the remaining AWGN and impulsive interference samples are still uncorrelated. Furthermore, both can be assumed to be Gaussian distributed in the frequency domain, even for small numbers of impulsive interference samples and for both considered interference models. This is explained by the noise bucket effect in [14]. In [13] it is shown that the ICI in the frequency domain is Gaussian distributed for sufficiently large numbers of sub-carriers N and uncorrelated blanking positions, i.e. Bernoulli-Gaussian noise. For Gated-Gaussian noise, it can be still assumed as an approximation. The expectation value of the useful OFDM signal power after the BN is constant for all sub-carriers, since on average each remaining sample comprises equal contributions from all sub-carriers.

For obtaining the SINR according to (7), we will now show[2] how to calculate P_{I}. This is followed by the derivation of the factor K.

Since the interference conditions may change over time we consider L OFDM symbols, comprising $N_L = L \cdot N$ samples, for calculating an adapted blanking threshold for this certain period of time. The choice of L depends on the type of interference and how fast the interference conditions vary. This issue will be discussed in Section V.

The following considerations are based on the assumption, that the OFDM signal in the time domain can be modeled as a complex Gaussian process with a Rayleigh distributed amplitude, which is valid for sufficiently large numbers of sub-carriers N [15].

A. Calculation of Remaining Interference Power P_{I}

For obtaining the remaining interference power P_{I} we will first calculate the expectation value of the total remaining energy $E_{\mathrm{w/I}}$ after the BN when blanking with a certain threshold T_{BN}. The probability density function (pdf) of the amplitudes of the received signal is denoted by $g(a)$ with amplitude $a = |r_{p,l}|$. Since in general the interference conditions, i.e. $g(a)$, are not known at the receiver, we propose to approximate $g(a)$ by the actual amplitude distribution of the N_L considered samples. The more OFDM symbols are taken into account, the more meaningful the approximated amplitude distribution will become, leading to a better estimate of the SINR. However, if the interference situation is differing significantly from one OFDM symbol to the next, separate thresholds for each OFDM symbol, i.e. $L = 1$, are more appropriate. This issue will be addressed in Section V. Now, based on $g(a)$, the total remaining energy $E_{\mathrm{w/I}}$ after the BN can be calculated by

$$E_{\mathrm{w/I}} = N_L \int_0^{T_{\mathrm{BN}}} a^2 g(a)\,\mathrm{d}a. \tag{8}$$

The total number of non-blanked samples N_{NB} within the L considered OFDM symbols is obtained by

$$N_{\mathrm{NB}} = N_L \int_0^{T_{\mathrm{BN}}} g(a)\,\mathrm{d}a. \tag{9}$$

Next, we are interested in the total energy $E_{\mathrm{wo/I}}$ of these N_{NB} samples without interference, i.e. the total remaining OFDM and AWGN signal energy after blanking. The exact value for $E_{\mathrm{wo/I}}$ cannot be calculated without any knowledge about the interference. However, it can be approximated based on the known amplitude pdf of the OFDM and the AWGN signal, i.e., if no interference is present. It is described by the Rayleigh distribution

$$f(a) = \frac{a}{\sigma^2} e^{-\frac{a^2}{2\sigma^2}}, \quad a \geq 0, \tag{10}$$

[2]In the following, we will write for clearness P_{I} and K instead of $P_{\mathrm{I}}(T_{\mathrm{BN}})$ and $K(T_{\mathrm{BN}})$.

with the constant value $\sigma = \sqrt{1/2 + \sigma_n^2}$. The expectation value of the power $P_{\mathrm{wo/I}}$ of a sample below T_{BN} without interference is now obtained when dividing the total energy by the number of respective samples. This is computed as

$$P_{\mathrm{wo/I}} = \frac{N_L \int_0^{T_{\mathrm{BN}}} a^2 f(a)\,\mathrm{d}a}{N_L \int_0^{T_{\mathrm{BN}}} f(a)\,\mathrm{d}a}. \tag{11}$$

Finally, to determine the total energy $E_{\mathrm{wo/I}}$ of N_{NB} samples we have to multiply the average power $P_{\mathrm{wo/I}}$ with the number of samples N_{NB}:

$$E_{\mathrm{wo/I}} = N_{\mathrm{NB}} \cdot P_{\mathrm{wo/I}}. \tag{12}$$

This approximation assumes that no sample with an OFDM signal and AWGN signal amplitude below T_{BN}, and each sample with an OFDM signal and AWGN signal amplitude above T_{BN}, is blanked. Apparently this is not true, since the impulsive interference may enlarge or reduce received sample amplitudes above or below T_{BN}. However, for a rare occurrence of impulsive interference or $\sigma_g \gg \sigma_n$ and $\sigma_g \gg \sigma_s$ this approximation is justified since the number of remaining samples after blanking comprising impulsive interference is small compared to the number of samples containing no impulsive interference.

As the impulsive interference spreads equally over all sub-carriers, the expected value for the remaining interference power P_{I} at a sub-carrier is then obtained by

$$P_{\mathrm{I}} = \frac{\left(E_{\mathrm{w/I}} - E_{\mathrm{wo/I}}\right)}{N_L}. \tag{13}$$

B. Calculation of Attenuation Factor K

Now we go on by calculating the factor K. We defined K as the ratio of the expected sub-carrier OFDM and AWGN power after and before the BN. Obviously, the sub-carrier OFDM and AWGN power before the BN is given by $(1 + N_0)$. The total remaining OFDM and AWGN signal energy after the BN $E_{\mathrm{wo/I}}$ has been calculated in (12). Since this total energy spreads equally over all sub-carriers, the remaining OFDM and AWGN power at a certain sub-carrier is obtained by dividing $E_{\mathrm{wo/I}}$ by the number of considered samples N_L. Thus K is computed as

$$K = \frac{E_{\mathrm{wo/I}}}{N_L(1 + N_0)}. \tag{14}$$

Note that in [13], K is defined as the ratio between the number of non-blanked samples per OFDM symbol and the number of total samples per OFDM symbol N. However, this is only an approximation when assuming that the blanking of a sample only depends on the impulsive interference, but not on the amplitude of the OFDM and AWGN signal. This approximation is justified if $\sigma_g \gg \sigma_n$ and $\sigma_g \gg \sigma_s$.

Taking (13) and (14) into account, we are now able to calculate the SINR based on (7). The optimal blanking threshold $T_{\mathrm{BN,opt}}$ is then obtained by finally applying (6). We will now go on by verifying the effectiveness of our proposed algorithm.

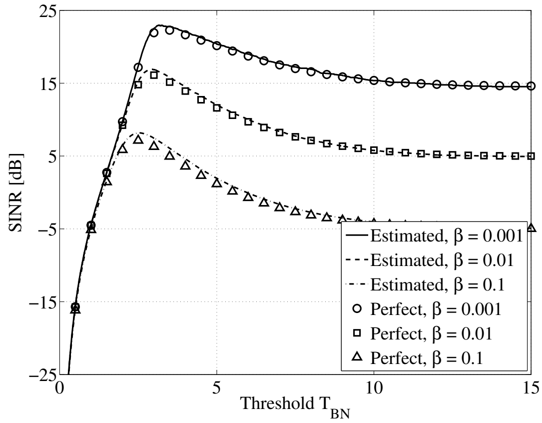

Fig. 2. SINR at the output of the BN versus threshold T_{BN} for Bernoulli-Gaussian noise, $\mathrm{SNR} = 25\,\mathrm{dB}$, $\mathrm{SIR} = -15\,\mathrm{dB}$.

IV. Comparison with Perfect Threshold

In this section, we will compare our proposed algorithm to the theoretically derived perfect calculation from [9] in terms of the SINR estimation, the determination of the threshold, and the influence on the performance by bit error rate (BER) simulations.

In Fig. 2, the SINR at the output of the BN is depicted versus T_{BN}, for Bernoulli-Gaussian noise with different values of β. We selected $N = 1024$, QPSK as modulation scheme, and no channel coding. The amplitude pdf $g(a)$ is approximated by the samples of $L = 500$ OFDM symbols at a time. As mentioned in Section II we consider only AWGN, but no fading or multipath channel is investigated. In the following, the signal-to-noise ratio (SNR) and the signal-to-interference ratio (SIR) are defined as

$$\mathrm{SNR} = \frac{1}{N_0}, \tag{15}$$

$$\mathrm{SIR} = \frac{1}{2\sigma_g^2}. \tag{16}$$

The results are compared to the theoretically perfect $\mathrm{SINR}_{\mathrm{perf}}$, which is calculated as in [9]. Note that the calculation of $\mathrm{SINR}_{\mathrm{perf}}$ is based on the knowledge of the interference parameters, i.e., β and σ_g. In contrast, our approach does not require the knowledge of the interference parameters. The estimated SINR matches the perfect case well and is only slightly above $\mathrm{SINR}_{\mathrm{perf}}$. In particular the position of the maximum is nearly the same with the perfect and our calculation, indicating a good estimate of $T_{\mathrm{BN,opt}}$. This issue will be analyzed in more detail in the next paragraph.

Next, we will examine the accuracy of the blanking threshold calculation. In Fig. 3, the calculated optimized threshold $T_{\mathrm{BN,opt}}$ and the theoretically perfect threshold $T_{\mathrm{BN,perf}}$ are plotted versus the SIR for $\mathrm{SNR} = 25\,\mathrm{dB}$. The other parameters are the same as above. Both $T_{\mathrm{BN,opt}}$ and $T_{\mathrm{BN,perf}}$ are derived by maximizing the respective SINR. Besides Bernoulli-Gaussian noise we also consider Gated-Gaussian noise with $\mu = 0.1$ and $\nu = 1$, corresponding to Bernoulli-Gaussian noise

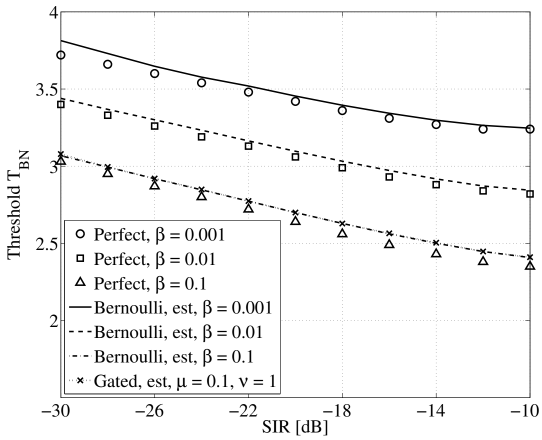

Fig. 3. Estimated and perfect blanking threshold versus SIR, $\mathrm{SNR} = 25\,\mathrm{dB}$.

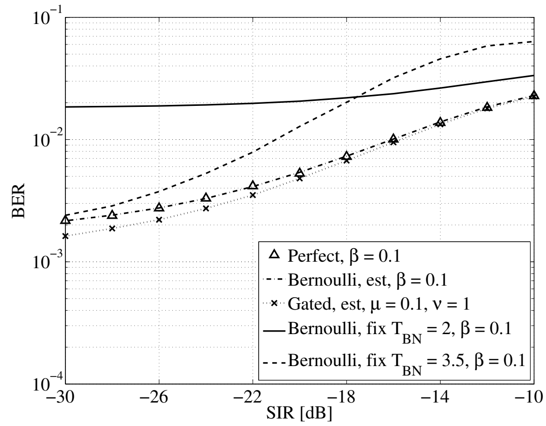

Fig. 4. Uncoded BER performance for fixed, estimated, and perfect blanking threshold versus SIR, $\mathrm{SNR} = 25\,\mathrm{dB}$.

with $\beta = 0.1$ in terms of the average number of interference samples. For Gated-Gaussian noise we obtain the same results as for Bernoulli-Gaussian noise. This is not surprising since the amplitude distribution does only depend on the number of interference samples but not on its positions, i.e., randomly spreaded or block-wise. Compared to the theoretically perfect threshold, $T_{\mathrm{BN,opt}}$ is slightly above $T_{\mathrm{BN,perf}}$. The little mismatch is probably a result of the approximation, which is used for calculating (12).

To evaluate the impact of the threshold mismatch on the system performance, the BER is selected as measuring metric. Therefore the BER is plotted versus the SIR in Fig. 4 for the same parameter set as above, with $\beta = 0.1$ for Bernoulli-Gaussian and $\mu = 0.1$ and $\nu = 1$ for Gated-Gaussian noise. To illustrate the influence of a poorly chosen blanking threshold, we added results for the case of a fixed threshold with different pre-defined values. It turns out that the little mismatch of $T_{\mathrm{BN,opt}}$ compared to $T_{\mathrm{BN,perf}}$ causes a negligible performance degradation for Bernoulli-Gaussian noise. For Gated-Gaussian noise, the BER is slightly below the Bernoulli-Gaussian case, especially for small SIR values. This is a consequence of the different types of interference models. While for Gated-Gaussian noise in each OFDM symbol exactly the same number of interference samples occur, Bernoulli-Gaussian noise defines only an occurrence probability leading to OFDM symbols comprising more interference samples than on average would occur. The latter leads to significantly more bit errors, compared to a fixed number of interference samples. This explains the inferior performance of Bernoulli-Gaussian noise compared to Gated-Gaussian noise. In contrast to an estimated threshold, a fixed threshold leads to a noticeable performance loss. This will become a severe problem especially when the interference situation changes during a transmission. In this case, our proposed threshold calculation performs superior, since for each set of L OFDM symbols a separate threshold is calculated. In other words the threshold calculation is adapted to each set of L OFDM symbols.

Note that in general the BER is getting lower when the SIR is getting smaller, i.e., the interference power is getting larger. This can be explained by the fact that a larger interference power leads to a higher blanking threshold, which reduces the probability of falsely blanking peaks of the OFDM signal.

V. Influence of interference and FFT size

Next, we will examine the dependency on the threshold calculation from the interference scenario. In particular, we are interested in the influence of the selection of L on the performance. In addition, we will have a look on the dependency of the performance on the FFT size N.

In our simulation we apply Gated-Gaussian noise with $\mathrm{SIR} = -15\,\mathrm{dB}$, $\mu = 0.2$ and $\nu = 10$. This model is compared to Bernoulli-Gaussian noise with $\mathrm{SIR} = -15\,\mathrm{dB}$ and $\beta = 0.02$, which leads to the same number of impulsive interference samples on average. In Fig. 5, we compare the BER for both interference scenarios. For deriving the blanking threshold, we implemented an OFDM symbol-wise threshold calculation ($L = 1$) and a joint threshold calculation for 500 OFDM symbols ($L = 500$). Both, $N = 1024$ and $N = 64$, QPSK modulation, and no channel coding were applied.

In general, the Bernoulli-Gaussian noise leads to a remarkably lower BER since the interference samples are spread over the received samples and do not appear bursty as in the Gated-Gaussian case. This is more suitable for the demodulation of the signals. One should mention that this drawback could be, at least partly, rectified by applying a bit interleaver in conjunction with channel coding. However, this would also blur the differences between an OFDM symbol-wise and a jointly blanking threshold calculation. Thus, it is omitted in our investigations.

As expected for Gated-Gaussian noise, i.e., strongly varying interference from one OFDM symbol to the next, an OFDM symbol-wise calculation leads to better results compared to the joint calculation. This does not hold for Bernoulli-Gaussian noise. In this case, the interference is nearly the same in each OFDM symbol and the joint threshold calculation benefits from a more reliable amplitude distribution of the received signal when taking more samples into account. Accordingly, in this case the joint calculation outperforms the symbol-wise

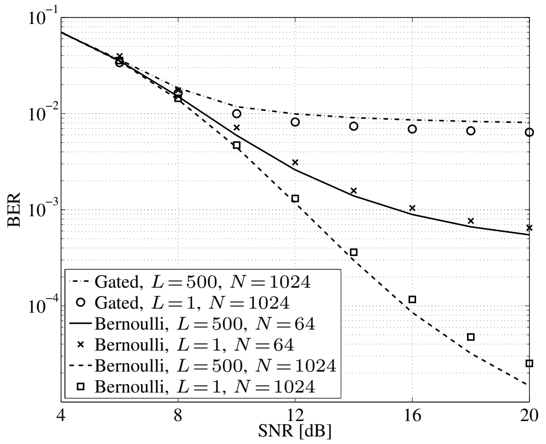

Fig. 5. Uncoded BER performance versus SNR for different FFT sizes and interference scenarios, $\mathrm{SIR} = -15\,\mathrm{dB}$.

calculation. The effect holds for both small and large FFT sizes.

For Bernoulli-Gaussian noise the FFT size has a strong impact on the BER performance. It degrades significantly when reducing N, both for small and large values of L. However, this is not particularly caused by a poor estimation of the blanking threshold. It rather occurs since assumptions concerning the Gaussian distribution of the remaining interference and induced ICI are no longer valid for small values of N. This behavior was also observed in [9].

VI. Conclusion

In this paper, we present a new method for optimizing the threshold for a blanking nonlinearity in OFDM systems. The algorithm does not depend on any knowledge of the impulsive interference the system is exposed to. We derive an expression for the threshold dependent SINR after the blanking nonlinearity. Its calculation is based on the amplitude distribution of the received samples. The expression for the SINR is maximized to obtain the optimal threshold. Simulations show that the performance loss compared to the theoretically derived perfect threshold is negligible. In addition, we also evaluated the influence of the FFT size and of the interference scenario on the performance of the proposed algorithm. It became clear that for Gated-Gaussian noise a separate threshold calculation for each OFDM symbol is superior, while for Bernoulli-Gaussian noise, especially for small FFT sizes, the threshold should be calculated jointly for multiple OFDM symbols.

References

[1] Y.H. Ma, P.L. So, and E. Gunawan, "Performance analysis of OFDM systems for broadband power line communications under impulsive noise and multipath effects," *IEEE Trans. Power Del.*, vol. 20, pp. 674–682, Apr. 2005.

[2] M. Ghosh, "Analysis of the effect of impulse noise on multicarrier and single carrier QAM systems," *IEEE Trans. Commun.*, vol. 4, pp. 145–147, Feb. 1996.

[3] D. Middleton, "Statistical-physical models of electromagnetic interference," *IEEE Trans. on Electromagn. Compat.*, vol. 19, pp. 106–127, Aug. 1977.

[4] J. Lago-Fernandez and J. Salter, "Modelling impulsive interference in DVB-T: Statistical analysis, test waveforms and receiver performance," *BBC R. and D. Whitepaper (WHP 80)*, Apr. 2004.

[5] Grace X. Gao, "DME/TACAN Interference and its Mitigation in L5/E5 Bands," in *ION Global Navigation Satellite Systems Conference*, Fort Worth, TX, USA, Sept. 2007.

[6] Sergey V. Zhidkov, "Analysis and Comparison of Several Simple Impulsive Noise Mitigation Schemes for OFDM Receivers," *IEEE Trans. Commun.*, vol. 56, pp. 5–9, Jan. 2008.

[7] H. A. Suraweera, C. Chai, J. Shentu, and J. Armstrong, "Analysis of impulse noise mitigation techniques for digital television systems," in *Proc. 8th Int. OFDM Workshop*, 2003, pp. 172–176.

[8] Chi-Hsiao Yih, "Iterative Interference Cancellation for OFDM Signals With Blanking Nonlinearity in Impulsive Noise Channels," *IEEE Signal Process. Lett.*, vol. 19, pp. 147–150, Mar. 2012.

[9] Sergey V. Zhidkov, "Performance Analysis and Optimization of OFDM Receiver With Blanking Nonlinearity in Impulsive Noise Environment," *IEEE Trans. Veh. Technol.*, vol. 55, pp. 234–242, Jan. 2006.

[10] J. Armstrong and H. A. Suraweera, "Decision Directed Impulse Noise Mitigation for OFDM in Frequency Selective Fading Channels," in *Proc. IEEE Global Telecomm. Conf.*, 2004, pp. 3536 – 3540.

[11] S.V. Zhidkov, "Impulsive noise suppression in OFDM-based communication systems," *IEEE Trans. Consum. Electron.*, vol. 49, pp. 944 – 948, Nov. 2003.

[12] S. Brandes, U. Epple, and M. Schnell, "Compensation of the Impact of Interference Mitigation by Pulse Blanking in OFDM Systems," in *Proc. IEEE Global Telecomm. Conf.*, 2009, pp. 1–6.

[13] U. Epple, K. Shibli, and M. Schnell, "Investigation of Blanking Nonlinearity in OFDM Systems," in *Proc. IEEE Int.Commun. Conf.*, 2011, pp. 1–5.

[14] H.A. Suraweera and J. Armstrong, "Noise bucket effect for impulse noise in OFDM," *Electron. Lett.*, vol. 40, pp. 1156–1157, Sept. 2004.

[15] P. Banelli and S. Cacopardi, "Theoretical analysis and performance of OFDM signals in nonlinear AWGN channels," *IEEE Trans. Commun.*, vol. 48, pp. 430–441, Mar. 2000.